AERO- HNSCC: An Autoencoder-Based Risk Stratification Model for Head and Neck Squamous Cell Carcinoma (2024)

Jucheng Hu

Abstract— **Head and neck squamous cell carcinoma (HNSCC) ranks among the deadliest cancers, with prognosis prediction remaining challenging due to the absence of reliable approaches. This study introduces a novel model, AutoEncoder Risk Stratification for Oncology in Head and Neck Squamous Cell Carcinoma (AERO-HNSCC), which transcends the traditional biomarker identification method by integrating multi-omics data for prognostic analysis of HNSCC. Our approach uniquely utilizes a deep autoencoder for pre-processing multi-dimensional data, including protein expression, RNA-Seq, and clinical information, enhancing the predictive accuracy of patient overall survival (OS). Developed and validated on The Cancer Genome Atlas (TCGA) HNSCC dataset, AERO-HNSCC demonstrates a significant success in risk stratification with an average precision of 73% and a statistically significant p-value of 0.0021 in the log-rank test for survival analysis. Compared with LASSO Cox Regression-based signature selection methods and raw multi-omics data for risk stratification, this new method shows comparable or superior performance. These quantitative evaluations demonstrate that the AERO-HNSCC encoded data establishes a robust association with patient OS and can accurately predict OS. In conclusion, this research contributes a novel computational framework for HNSCC prognosis, its success underlines the potential for such models to transcend traditional biomarker discovery and to offer broader, more universal solutions in oncological research.**

Index Terms—**hypoxia, immune, gene signature, tumour, cancer, microenvironment, machine learning, deep learning, autoencoder, prognosis, multi-omics, head and neck squamous cell carcinoma**

I. INTRODUCTION

HNSCC is squamous cell carcinomas arising from lesions in the head and neck region, including the oral cavity, tongue, nasal and paranasal cavity, pharynx, and larynx[1]. HNSCC is among the top ten leading causes of cancer worldwide, with approximately 500,000 new cases diagnosed annually[2]. The high prevalence and risk associated with HNSCC emphasize the importance of developing effective methods to assess cancer progression and predict patient prognosis.

Numerous studies have developed various biomarkers with prognostic value for HNSCC. Among all these biomarkers, gene signatures, particularly the Hypoxia Signature (HS) – a set of differentially expressed genes (DEGs) under hypoxic conditions within the tumour microenvironment – have emerged as a key method. The expression level of HS can be used to infer intratumoural hypoxia levels[3], which is crucial for predicting clinical outcomes[4]. This signature-identification-centred (SIC) method also applied on protein expression data. It has been shown that proteomic biomarkers can function as predictor for cancer diagnosis and prognosis [5], and some proteomic signature has been developed on the Reverse Phase Protein Array (RPPA) data[2].

Despite these advances, challenges remain, particularly in harnessing the full potential of integrated data from various omics studies (multi-omics data), due to its increasing dimensionality. This complexity complicates the extraction of meaningful information from the noise. AEs have been introduced as a solution to the dimensionality problem have been introduced as a solution to this dimensionality problem and offer a novel approach beyond traditional signature identification methods. Instead of developing prognostic signatures, AE-based methods aim to capture insights from the entire dataset. However, existing works either rely on supervised method[6], which may not be feasible when labels are unavailable, or are lacking application to protein expression data[7], or do not specifically focus on HNSCC[8].

These research gap necessitates this research, and leads to the objective of this research: firstly, determine whether protein expression data can provide insights into HNSCC patient OS and develop an AE-based risk stratification model for accurate OS classification and therefore enabling early identification of high-risk patients.

The structure of this paper is as follows: Section 2 reviews the related work in the field, providing context and highlighting the novelty of our approach. Section 3 delves into the experimental design, detailing the AERO-HNSCC architecture, data preparation procedures, validation metrics, and benchmarking strategies. Section 4 analyses the results, assessing the efficacy and potential implications of our model. In Section 5 we discuss the limitation of current work and lead to the final Section 6, suggesting directions for future research.

II. RELATED WORK

The Related Work section of this paper delves into two pivotal methodologies that have significantly impacted the prognosis and classification of HNSCC: SIC Methods and AE-Based Methods. Understanding these approaches illuminates the backdrop against which this research is situated.

A. SIC Methods

SIC methods have been cornerstone approaches in deciphering the complex molecular landscapes of cancers, including HNSCC. These methods focus on identifying specific gene signatures that correlate with disease outcomes, HSs especially. All SIC-related paper reviewed are shown in table I.

TABLE I
Methods and Tumour Type of Reviewed Papers

First Author	Year	Methods	Tumour
Cheng-Peng Gui	2021	t-SNE and Lasso	crCC
Yifan Liu	2020	t-SNE and Lasso Cox Regression	Gastric Cancer
Zhi Liu	2021	LASSO	BLCA
Yanhong Shou	2021	LASSO	Melanoma
Jinman Zhong	2021	LASSO	AML
Xia Yang	2021	LASSO	Breast cancer
Ke Wang	2022	LASSO	GBM
Chenyu Nie	2022	LASSO	Cervical Cancer
Xiong Tian	2022	LASSO	PAAD
Fanhong Zeng	2021	K-mean	HCC
Brian Lane	2022	K-mean	LUDA
Jun Shao	2021	K-mean and LASSO Cox Regression	LUAD
Jill M. Brooks	2019	Unsupervised Hierarchical Clustering	HNSCC
Jia Li	2022	Random Forest	Breast Cancer
Donglei Wu	2020	LASSO Cox Regression	HNSCC
Baohui Zhang	2020	LASSO Cox Regression	HCC
Run Shi	2021	LASSO Cox Regression	LUDA
Dongjie Chen	2021	LASSO Cox Regression	PDAC
Qiangnu Zhang	2021	LASSO Cox Regression	HCC
Xiangqian Zhang	2023	LASSO Cox regression	Gastric Cancer

As a conclusion from the papers listed above, the development of HS can be generalized as a three-stage process for various tumour types:

1) **Identification of Hypoxia DEGs**
   This initial step involves obtaining all hypoxia-related DEGs, which can be sourced through literature reviews[9], databases[10], or clustering by algorithms like K-mean[11-13] or UHC[9].
2) **Feature Selection on DEGs**
   Subsequently, apply feature selection by conducting LASSO[10, 14-20], LASSO Cox Regression[21-25], or Random Forest[26] on DEGs to filter prognostic HSs.
3) **Prognostic Model Development**
   The final step involves developing a prognostic model, which may take the form of a score or a more complex model incorporating additional features.

Specifically, while all other works focus on gene expression datasets, Wu et al.'s work[2], following the identical three-stage process, but developed a proteomic signature on the TCGN-HNCC RPPA dataset, achieved a 0.779 of area under the curve (AUC) of the corresponding receiver operating characteristic (ROC) in the task of classifying patients into high and low-risk groups.

Due to the variance in cancers, datasets used for HSs development, the result measurement and processes of HS identification, conducting comparative research on the performances of all different methods remains challenging. Noting the overlapping focus on Hepatocellular Carcinoma (HCC) and Lung Adenocarcinoma (LUAD), this research will focus on the performance of 6 works that developed HSs for these two tumours, respectively.

As shown in table I, three studies centred on HCC. Zeng et al.[12] apply the K-mean in stage 1, the Identification of Hypoxia DEGs, leading to the discovery of four genes: DCN, DDIT4, NDRG1, and PRKCA from the ICGC dataset. Their hypoxia-risk model demonstrated highest accuracy among all three HCC studies in predicting one-year and three-year OS. The AUC values for one-year, tow-year and three-year OS are 0.809, 0.771, and 0.791, respectively.

Zhang et al.[22] employed LASSO Cox Regression for stage 2 the Feature Selection on DEGs. This approach identified a HS of another 21 distinct genes, including ADM, BNIP3, BNIP3L, and CA9. AUC values for one, three, and five years were 0.71, 0.73, and 0.69, respectively.

Another Zhang et al.[13] integrated both K-mean and LASSO Cox Regression in stage 1 and 2, uncovering three significant genes: PDSS1, SLC7A11, and CDCA8. The AUCs for half-year, one-year, three-year, and five-year OS were 0.76, 0.78, 0.7, and 0.7, respectively.

Shifting the focus to LUDA, there are three studies. Lane et al.[11], following a similar approach to Zeng et al.[12], constructed a 28-gene hypoxia signature from the TCGA-LUAD dataset, using K-mean in stage 1. Their research emphasized qualitative validation, employing the Hazard Ratio (HR), Confidence Interval (CI), and Kaplan-Meier analysis p-values as metrics. The prognostic relevance of their signature for OS was substantiated in independent cohorts from the TCGA-test and GEO datasets, showcasing results of HR 1.76, CI 1.50–2.08, and $p < 0.0001$.

Mirroring the methodology of Zhang et al.[22], Shi et al.[21] identified 10 genes using LASSO Cox Regression in the feature selection stage. The HS is developed from the GEO GSE72094 dataset and validated on datasets from U133A, U133 Plus 2.0 and TCGA with result HR = 6.738, 95% CI = 3.902-11.64 and p = 6.42e-09.

Lastly, Shao et al.[10] formulated a seven lncRNA HS from a combination of 13 microarray datasets from various platforms and one RNA-Seq dataset from TCGA. K-mean and Lasso cox regression is used in stage 1 and 2 respectively. This signature was validated on the TCGA validation set, achieving AUC values of 0.665, 0.693, and 0.652 for 1-, 3-, and 5-year overall

survival, respectively. Though the main paper did not provide detailed HR, CI and p-value result, supplementary documents provide a separated Kaplan-Meier analysis result for all seven gens, with HR ranging from 0.61 to 1.65, CI from 0.42-0.88 to 1.39-1.95 and p-value from less than 0.001 to 0.277.

Despite their proven utility in numerous studies, SIC methods often fall short in addressing the multifaceted nature of cancer progression, exhibit a lack of universality. The process of obtaining hypoxia DEGs relies on existing knowledge of specific genes[9] or proteins[2]. Moreover, when transitioning from one type of cancer to another, the resulting signature[13, 21] could be completely distinct , with the number of genes in the HS varying considerably. Even within the same cancer type, the developed HS[12, 22] can be markedly different when different datasets or methodologies are employed. Furthermore, a comparison between methods that achieved the highest accuracy for LUAD and HCC[12, 21] reveals a plethora of approaches to developing HS, yet there is no clear, universally superior approach that performs optimally across all cancer types. This inconsistency and limitation lead researchers to seek more integrative and comprehensive approaches.

B. AE-Based Methods

In contrast to SIC methods, AE-Based Methods offer a fresh perspective on data analysis in oncological research, particularly through the lens of multi-omics integration. This shift is due to the complexities of cancer that extend beyond linear biomarker associations, emphasizing the potential of non-linear data relationships and the holistic nature of biological systems. Current works can be divided into two paths: supervised and unsupervised.

1) Supervised Approaches

Tan et al.'s work[6] focused on pan-cancer multi-omics datasets, constructing individual autoencoders for each data type—ranging from DNA methylation to protein expression. By encoding these varied data types to a uniform dimensionality and training with distinct labels such as OS and disease-specific survival (DSS), their approach achieved a noteworthy AUC of 0.7830 for binary classification.

Similarly, Mondol et al.[8] presented a blend of unsupervised pre-training with supervised fine-tuning through an adversarial autoencoder and a method named 'TopGene.' This approach identifies significant genes within the latent space, demonstrating high precision of 0.8596 in classifying sub-types of breast cancer.

Madhumita and Sushmita's[27] work not quantified through AUC or precision metrics, since they focused on the subtype clustering of glioblastoma multiforme (GBM). They contribute a method that performs supervised feature selection before training a sparse autoencoder.

2) Unsupervised Approaches

On the unsupervised side, AE-Based Methods demonstrate their strength in survival stratification without the prerequisite of predefined labels. Song et al.'s research[7] in colorectal cancer utilized DNA methylation, RNA-Seq, and miRNA-Seq data with a deep sparse AE, achieving a concordance index (C-index) of 0.781 in survival analysis.

Ellen et al.[28] constructed a single-layer denoising autoencoder that integrates mRNA, miRNA, DNA methylation, and long non-coding RNA data, yielding C-index of 0.69 ± 0.03 for LUAD in survival analysis .

Arafa et al.'s work[29] with a Reduced Noise Autoencoder showcases the utility of AE in enhancing data quality through noise reduction. Utilizing a three-layer AE with Reduced Noise-Synthesis Minority Over Sampling Technique (RN-SMOTE), they achieved a precision of 0.75 on a colon cancer dataset in cancer sub-type binary classification using only genomic data.

3) Transition and Comparative Outlook

AE-Based Methods are forging new paths in cancer research, they stand in stark contrast to SIC Methods by offering a more flexible and comprehensive approach to construct association with clinical endpoints and multi-omics data. Characterized by their ability to handle high-dimensional data and applicable to various cancer types without the need for prior biological knowledge, these methods uncover complex, non-linear relationships that traditional methods might overlook. As this research transitions from the specificities of SIC Methods to the broad potential of AE-Based Methods, it becomes evident that the latter may offer a more integrative and universal framework for understanding the multifaceted nature of cancer progression and patient prognosis.

Despite the innovative strides made by AE-Based Methods in oncological research, certain limitations persist, guiding the direction of our work. Firstly, while supervised methods have demonstrated utility in model architecture and insights, their reliance on labelled data contradicts the growing need for more universal, label-independent approaches in the field. This dependency limits their applicability in situations where comprehensive labelling is impractical or not available, underscoring the necessity for advancements in unsupervised learning techniques. Moreover, a significant gap in the literature is the lack of unsupervised AE applications specifically targeting HNSCC. Notably absent are studies that integrate protein expression data with autoencoders to predict OS in HNSCC patients, an area ripe for exploration. Our research aims to bridge these gaps by developing an unsupervised AE approach that not only transcends the need for labelled data but also focuses specifically on the integration of protein expression to enhance the prognostic understanding of HNSCC. In doing so, we aspire to create a more versatile and comprehensive tool for cancer prognosis, moving beyond the constraints of current methodologies to better meet the complex demands of oncological data analysis.

III. Experiment Design

A. Methodology

In this study, we employ a strategic approach by iteratively applying a series of AEs, specifically optimized for protein

expression datasets. This methodology is based on the hypothesis that the intricate biological signals embedded within protein expression data can be more effectively decoded and utilized through a tailored and well-optimized AE. We iterate across a spectrum of AE architectures, with each iteration designed to capture more significant OS signal from the protein expression data. This series of AEs allows for comprehensive exploration beyond surface-level patterns, delving into deeper, potentially uncharted biological signals that could play a pivotal role in HNSCC prognosis.

Each AE in our iterative series is meticulously constructed and optimized, with the number of nodes in each layer and bottleneck customized to match the specific dimensions and characteristics of protein expression datasets. This optimization process is critical as it balances the complexity required to model biological intricacies against the risk of overfitting, ensuring that each AE captures genuine reproducible patterns.

The iterative nature of our approach not only enhances model robustness through continuous refinement but also enables comparative analysis among different AE architectures. This comparison is vital for identifying the most effective models in encoding significant prognostic features from protein expression data, ultimately aiming to improve accuracy and reliability in HNSCC prognosis.

B. AERO- HNSCC Architecture

1) Initial Autoencoder Architecture

The foundational architecture begins with a standard Autoencoder (AE) designed to process input layers consisting of 468 nodes, each representing a unique protein expression. The network architecture flows from the input layer into two hidden layers of sizes 64 and 32, respectively, utilizing the Rectified Linear Unit (ReLU) activation function to introduce non-linearity and aid in the learning process. The output layer applies a sigmoid activation function to ensure the output values are normalized between 0 and 1, mirroring the input data's format. This structure is optimized with the Mean Squared Error (MSE), serving as the reconstruction loss function to gauge the network's performance in accurately reconstructing the input data. To explore the optimal compression and feature extraction capabilities, this AE is trained with three variations, featuring bottlenecks of sizes 2, 6, and 12.

2) Transition to a Wider Deep Autoencoder (DAE)

Acknowledging the necessity for higher-dimensional representations to adequately capture the OS signal, we next introduce a wider and deeper Autoencoder (DAE). This enhanced model connects the input layer to three subsequent hidden layers sized at 256, 128, and 64, maintaining the ReLU activation function for these layers. The remaining settings, including the Adam optimizer and MSE loss, are preserved from the initial AE design. The DAE undergoes training across a range of bottleneck sizes - 12, 48, 36, 34, 32, 28, 24, and 18 - with empirical results indicating that setting the bottleneck to 18 yields the highest precision in capturing the OS signal.

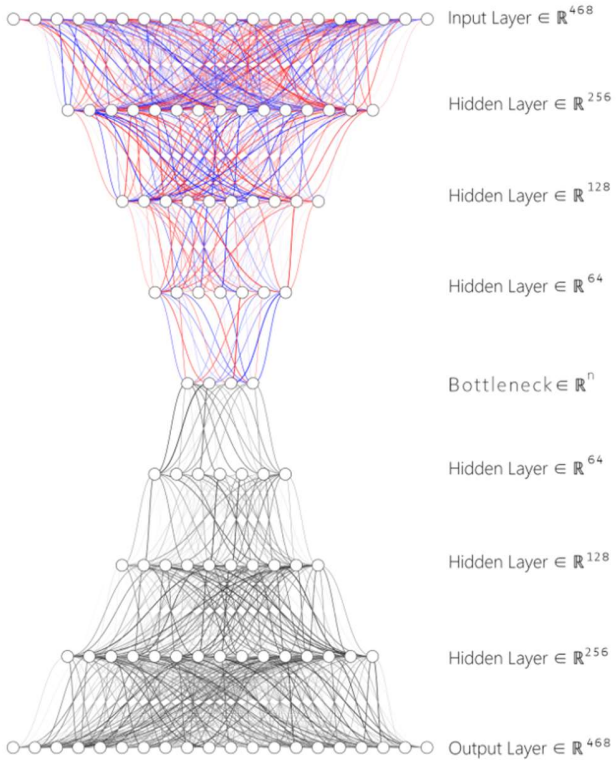

Fig.1. SDAE Architecture, Applied L1 Regularization on Encoder Layers

3) Incorporating Sparsity: Sparse AE (SAE) and Sparse DAE (SDAE)

Building on these findings, we further modify the initial AE into a Sparse AE (SAE) by incorporating L1 regularization on its hidden layers, with a penalty rate of 1e-6. This addition encourages the model to learn sparser representations of the data, potentially enhancing its interpretability and efficiency in capturing relevant features. Observing noticeable improvements with this modification, we extend the regularization to the DAE, transforming it into a Sparse DAE (SDAE), as shown in Fig 1. This adaptation applies the same L1 regularization technique to the DAE's hidden layers, trying to refine the model's performance further.

4) Integration with Classifier Systems

Upon the training completion of each AE variant, the encoded data undergo a subsequent layer of analysis involving Principal Component Analysis (PCA), K-means clustering, Random Forest Classification, and Support Vector Machine (SVM) to test performance metrics, as shown in Fig 2. This two-tiered approach, pairing each AE with robust classification methods, combined to our AERO-HNSCC model. This integrated system aims to refine and validate the predictive power of the encoded features, focusing on the accuracy and efficacy in stratifying patient outcomes based on protein expression profiles. This dual-phase methodology—merging deep learning-based feature extraction with conventional classification techniques—establishes a comprehensive

framework for advancing the prognostic analysis in HNSCC.

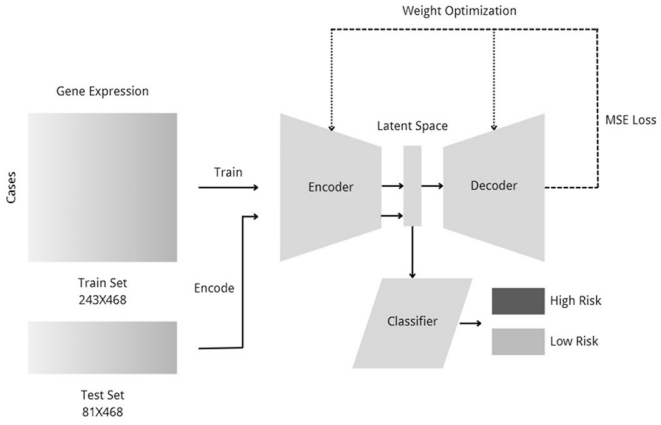

Fig.2. AERO- HNSCC Architecture

B. *Dataset Description and Process*

The AERO-HNSCC is developed on the TCGN-HNSCC RPPA dataset, comprising 353 individual TSV files. Each file corresponds to a distinct patient case, encapsulating a diverse array of 487 protein expressions. The overall data process pipeline is illustrated in Fig 3.

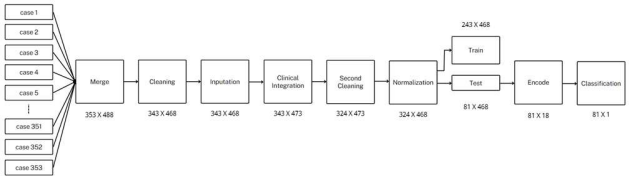

Fig.3. Data Processing Flow Chart

Upon examination, several issues were identified within the merged dataset: 18 columns contained NaN (not a number) values, one column was missing in 280 cases, and 10 cases were found to be missing data across 218 columns. Due to the significant proportion of missing information, these entries were excluded from further analysis. The refined DataFrame then revealed an additional 141 cases with 12 columns of missing data. Given the scale of the dataset (468 total protein expression columns) and the relatively small number of missing columns, we opted for a targeted imputation strategy by incorporating clinical data.

Clinical information was integrated with the RPPA dataset using the 'case_submitter_id,' a unique identifier for each patient, enabling a direct correlation between clinical and protein expression data. Then, a target-encoding-like imputation strategy is used. Cases without missing values were grouped based on their AJCC pathologic stage, and the median values for the 12 incomplete columns were calculated for each group. By introducing new information from other omics dataset, this median-based imputation ensured a robust and informative dataset.

A subsequent round of filtering was conducted to remove two additional cases with ambiguous OS information, resulting in a finalized dataset comprising 324 cases, each characterized by 468 protein expression columns, as depicted in Supplementary Figure 1.

Normalization of the protein expression data was then addressed, as highlighted in Fig 4. Given the observed variance in protein expression means, ranging from 2 to 0.001, normalization was deemed essential. According to Hoffer et al.[30], this step is curtail to improves the gradient flow, ensuring that all input features contribute equally and effectively during the learning process, which leads to faster and more stable convergence.

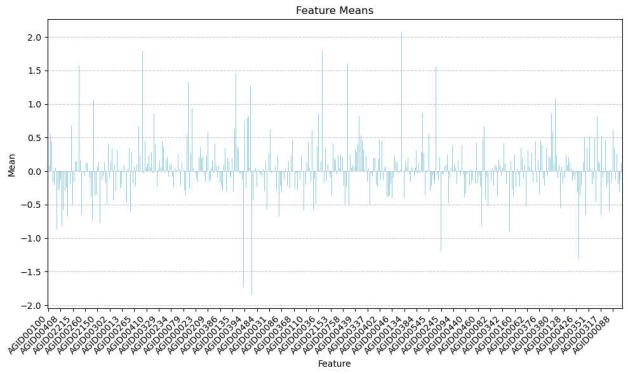

Fig.4. Protein Expression Means Scatter Graph

The final step in the data processing involves remapping the OS for each patient. Depending on the 'vital_status', labels such as 'dead within 10 years' and 'alive or dead after 10 years' are generated from clinical features such as 'days_to_death' and 'days_to_last_follow_up'. By grouping the patients into categories of 'alive longer than 10 years' (low risk) and 'alive less than 10 years' (high risk), we balance the population of each group to ensure unbiased classification results.

D. *Training*

For each AE variant within our series, the Adam optimizer was employed due to its proven efficiency in handling sparse gradients and its adaptability in learning rates, making it an ideal choice for our complex dataset. To closely monitor the model's performance and generalize its applicability, we attached the test set as our validation data without extra validation set. This strategy was adopted due to dataset size constraints and aimed to maximize the usage of all available data, allowed us to directly observe the model's predictive capabilities on unseen data after each training epoch.

Notice that the loss sometimes goes up in some last epochs, we implemented a checkpoint system. This system was designed to save the model's state at the epoch which demonstrated the highest performance on the test set. Such a method ensured that we retained the most effective version of the AE, even if the model's turns to overfit one the training set and the performance fluctuated in subsequent epochs.

The training regimen was set to run for 100 epochs for each AE, with a batch size of 8. This relatively small batch size was chosen to enhance the model's ability to learn from the

dataset intricately, allowing for finer adjustments to the weights and biases during the optimization process.

Throughout the training process, we meticulously tracked the loss for each AE. The MSE loss function was used to quantify the discrepancy between the original input data and the reconstructed output from the AE. This loss metric provided us with a direct measure of the model's reconstruction accuracy, serving as a critical indicator of the AE's performance.

To facilitate a comprehensive analysis of the training outcomes and loss trends across epochs, the loss metrics obtained for each AE were plotted in Supplementary Figure 2. This visualization aids in assessing the training process's effectiveness, showcasing the progression of model optimization over time.

In total, 15 AEs are trained, including two extra that used the initial architecture, the loss in the training is plotted in the supplementary table I. They were trained on datasets without imputed columns, featuring a bottleneck of size 6. These two additional AEs were utilized to validate the performance of the imputation.

E. Metrics

The success of the training process for the AEs and classifiers was evaluated using distinct, targeted metrics, designed to the research objectives and functionalities of each component, some of them also applied for benchmarks.

For the AEs, the primary metrics were reconstruction loss and validation loss. The reconstruction loss measures the difference between the original input and the reconstructed output produced by the autoencoder, providing an indication of how well the AE can replicate the input data after compression and decompression processes. This metric is crucial for assessing the AE's ability to capture the underlying data structure effectively. The validation loss, on the other hand, is computed on a separate set of data not seen by the model during training, offering insight into the model's generalization capabilities and helping to prevent overfitting.

The performance of the classifiers was evaluated using precision, recall, and the F1-score, and the confusion matrix. Precision measures the proportion of correctly identified positive outcomes from all predicted positive outcomes, providing insight into the model's ability to minimize false positives. Recall, or sensitivity, assesses the proportion of actual positive outcomes correctly identified by the model, highlighting its ability to minimize false negatives. The F1-score is the harmonic mean of precision and recall, offering a single metric that balances both concerns, particularly useful when dealing with imbalanced classes. When compared with other studies, the confusion matrix is converted into an equivalent AUC of the ROC for direct comparison with benchmarks.

For the validation of the AERO-HSNCC framework, the Kaplan-Meier Survival Curve and the log-rank test were utilized as key metrics. The Kaplan-Meier Survival Curve offered a visual and statistical representation of the time-to-event data, allowing for an intuitive understanding of survival probabilities over time across different groups. The log-rank test provided a method to statistically compare the survival distributions of two or more groups, making it an essential tool for assessing the significance of differences observed in the survival curves. Together, these metrics provided a comprehensive view of the AERO-HSNCC framework's ability to distinguish between different prognostic outcomes, contributing to a robust evaluation of the models' performance in a clinical context.

F. Benchmarks

The benchmarking of our experimental design is set against three pivotal and state-of-the-art studies that epitomize the forefront of predictive modelling in HNSCC and related areas. These benchmarks were selected for their relevance in terms of topic, data, and methodologies and include both traditional SIG methods and AE-based approaches.

Brooks et al.[9] developed a gene signature through SIG method specifically for HNSCC. Their validation in two cohorts resulted in log-rank test p-values of 0.5 and 0.2, respectively. They concluded that the HNSCC gene signature was not independently prognostic based on these outcomes. Their work is a critical reference in the field, demonstrating the application of traditional SIG methods to develop gene signatures for prognostic analysis. It provides a gene-centric benchmark against which we can compare the prognostic utility of our model, particularly through the association between the encoded data and OS via the log-rank test result.

Wu et al.[2] validated a SIG method developed proteomic signature for HNSCC. Their work achieved an AUC of 0.779 in ROC analysis, indicating significant prognostic capability. As a proteome-focused study, this provides a vital comparison point for assessing the predictive power of our model through AUC.

Tan et al.[6] developed a pan-cancer AE-based method for OS prediction. While not exclusively focused on HNSCC, their results are referable as HNSCC is included. Their supervised model achieved an AUC of 0.7830, underscoring the potential of AE-based methods in cancer prognosis across various types. This benchmark is invaluable for contrasting the generalizability and effectiveness of AE-based models, including in HNSCC contexts. It offers insights into the broader applicability of our methods in oncological research.

Our experimental design will be rigorously evaluated against these benchmarks to determine the advancements our model brings in predictive accuracy, prognostic significance, and methodological innovation in the realm of HNSCC prognostication. The chosen metrics, including log-rank test p-values for survival analysis and AUC for predictive accuracy, form a comprehensive framework for this comparison. These benchmarks not only highlight progress within the domain but also guide our ongoing efforts to refine and enhance prognostic models for HNSCC and beyond.

IV. Analysis of Results

A. Interpretation of Findings

As the initial step and primary objective of this research, and outlined in the introduction, the first task was to examine whether protein expression data contain insights into HNSCC OS. Therefore, following the acquisition and cleaning of the RPPA data, we conducted an exploratory classification using SVM with a linear kernel. The accuracy for this binary

classification was 0.58, significantly surpassing the 50% threshold. This positive signal led us to further investigation.

Subsequently, we trained the first four AEs. The initial architecture AEs encoded all 468 proteins into dimensions of 6 and 2, with and without the imputation columns. By including the imputation, we observed an 8.51% and 4.08% increase in accuracy, respectively, thereby validating the effectiveness of the imputation approach. However, the highest result obtained with the imputed data encoded to 6 dimensions was 0.59, showing no substantial improvement compared to the raw RPPA data. Visualization was performed by applying PCA with components of 3 and 2 to the six-dimensional results, and plotting the encoded two-dimensional data, as illustrated in Fig 5, revealed no clear boundaries between the two risk groups. Observing the minimal improvement when scaling up to six dimensions, we hypothesized that the AE might require more dimensions to capture the pattern effectively. Consequently, we trained another AE with a 12-dimensional output. Here, approaching the upper limit of hidden layer size, we explored whether performance could be further enhanced by a wider and deeper AE. We thus designed and trained eight variations of the DAE with different bottlenecks, decreasing from 48. The optimal performance was achieved with a bottleneck size of 18, which resulted in a precision of 0.73, and was finalized as the AE of the AERO- HNSCC. The confusion matrix for this DAE is displayed in Figure 6.

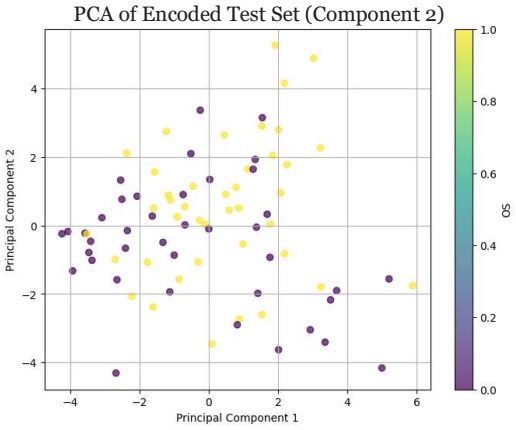

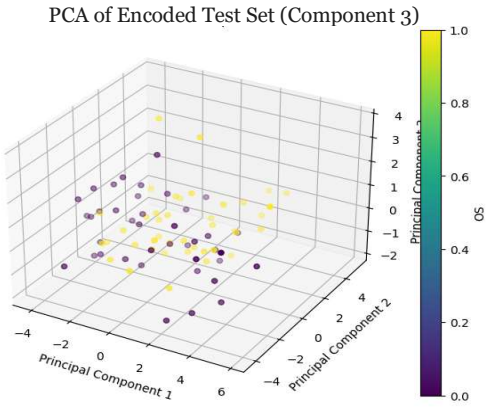

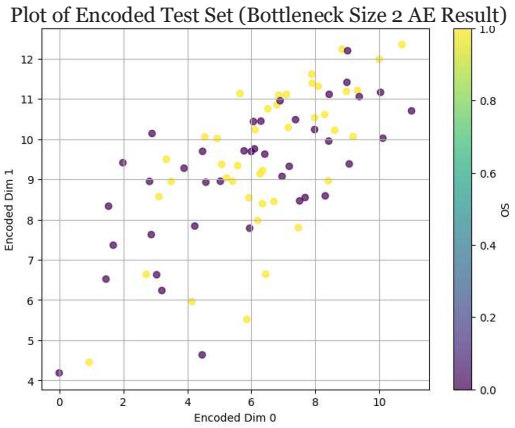

Fig.5. Encoded Test Set Visualization

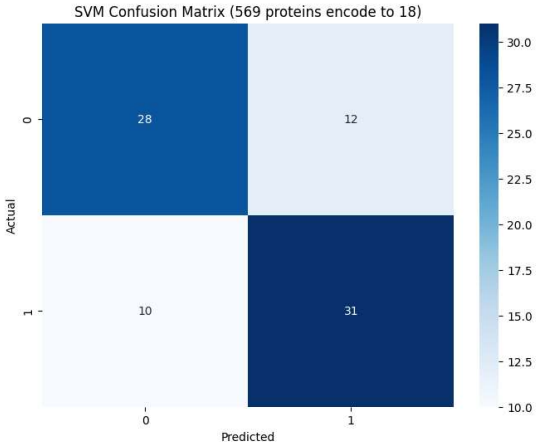

Fig.6. Confusion Matrix of the DAE Bottleneck Size 18

Obtained the AERO- HNSCC AE, we proceeded to assess the prognostic significance of the encoded features using survival analysis techniques. Specifically, we plotted the Kaplan-Meier Survival Curve to visually represent the survival probabilities of patients stratified based on the risk groups identified by our model. This visualization, as demonstrated in Figure 7, provides a clear, graphical representation of the survival distributions, allowing for an intuitive understanding of the differences between the high-risk and low-risk groups identified by the AERO-HNSCC model.

To statistically validate the distinctions observed between these groups, we employed the log-rank test. This non-parametric test is utilized to compare the survival distributions of two or more groups and is a standard method in survival analysis to assess the statistical significance of differences between the Kaplan-Meier curves. The result of the log-rank test, with a p-value of 0.0021, indicates a statistically significant difference in survival rates between the groups. This significant p-value underscores the prognostic relevance of the patterns captured by our Autoencoder model, suggesting that the encoded features have substantial implications for predicting patient outcomes in HNSCC.

In the following research we also tested the performance of SAE and SDAE, although by apply L1 regularization we do

observe a more stable AE performance, it does not improve the performance of classification.

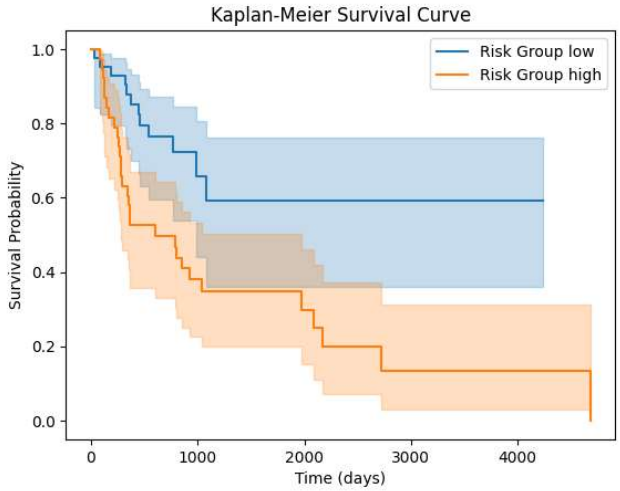

Fig.7. Kaplan-Meier Survival Curve Graph

B. Benchmark Comparison

Brooks et al.'s HNSCC HS study[9] concluded that the HS did not possess independent prognostic value. In contrast, the AERO-HNSCC model's log-rank test result, with a significantly lower p-value of 0.0021, suggests a strong association between the encoded data and OS, thereby indicating an improvement over traditional SIG methods in prognostic analyses. This outcome underscores the AERO-HNSCC model's potential as a more effective tool for prognosis in HNSCC.

Wu et al.[2] explored the prognostic capabilities of a proteomic signature developed through SIG methods, achieving an AUC of 0.779 in their ROC analysis. This sets a critical benchmark for our model. By constructing the AUC from the confusion matrix, our AERO-HNSCC model achieved an AUC of 0.73 in identifying high-risk and low-risk groups, demonstrating comparable performance. When using the proteomic signature they developed directly in the classification, we achieved an accuracy of 0.59, which is significantly lower than AERO-HNSCC's 0.73, showcasing better performance by AERO-HNSCC in direct classification tasks.

Tan et al.[6] conducted a broader study with their pan-cancer AE-based method, inclusive of HNSCC, achieving an AUC of 0.7830. This figure is 6.85% higher than that of AERO-HNSCC. Given their use of more omics data and a supervised method, this difference is within expected bounds. However, the AERO-HNSCC model still presents significant applicability and effectiveness, particularly considering its focus on HNSCC and utilization in an unsupervised context.

In each of these comparisons, our AERO-HNSCC model demonstrates substantial merit, either by showcasing improvements over traditional methods or by providing competitive performance against more generalized approaches.

V. Discussion & Limitations

The AERO-HNSCC illustrates a significant step forward in utilizing autoencoder-based methodologies for oncological prognostication. However, the shift towards SAE or SDAE did not yield the anticipated improvements. This could be attributed to the specific nature of SAEs, which are designed to address high-dimensionality issues primarily in datasets with a larger feature-to-case ratio. Given that the RPPA data comprises 468 protein expressions across 324 cases, the structure may not have been optimal for SAE application, possibly due to an insufficient level of inherent sparsity or noise within the dataset.

Another limitation of current AERO-HNSCC is developed on the dataset of one single type of cancer, which restricts the case diversity and number. Expanding the application to multiple cancers could offer a richer dataset, potentially enhancing the AE's learning capability and overall model performance.

VI. Conclusion and Future Work

The AERO-HNSCC workflow is designed to operate independently, relying solely on multi-omics datasets. This autonomous design not only streamlines its application but also holds potential to extend its utility beyond existing limitations. Unlike approaches that require detailed knowledge of specific genes or proteins, AERO-HNSCC could aid in uncovering new oncological biomarkers, as demonstrated by the "TopGene" methodology developed by Mondol et al.[8].

Building on the findings of Tan et al.[6], we have validated the efficacy of AE in analysing pan-cancer datasets. Given the inherent capabilities of AEs, there is a promising avenue for AERO-HNSCC to be applicable across a range of cancer types, potentially evolving into a universal tool for cancer analysis. However, this hypothesis requires thorough future investigations for comprehensive validation. Currently, our focus on a single cancer type limits the diversity of cases. Expanding this scope to include multiple cancer types could significantly increase the dataset size, thereby enhancing the AE's ability to learn more accurate data representations and potentially improving overall performance.

Furthermore, there is an opportunity to integrate additional multi-omics data into AERO-HNSCC. At present, the system utilizes only clinical and protein expression data. Echoing the approach by Tan et al.[6], we propose developing distinct AEs for each omics type and then combining these for classification. Although Tan et al. assumed equal informational value across different omics dimensions—an assumption yet to be confirmed—their framework for omics integration merits further investigation.

While the current research phase does not allow for direct performance comparisons due to the distinct cancer types focus, determining the specific performance impact of denoising AEs on HNSCC remains challenging. Future versions of AERO-HNSCC could benefit from integrating denoising techniques to enhance model accuracy. Moreover, given the balanced sample of survival outcomes in HNSCC, extending our approach to include additional cancer types with diverse survival outcomes might necessitate adaptive sampling techniques, such as RN-SMOTE introduced by Arafa et al.[29], to ensure methodological soundness.

APPENDIX

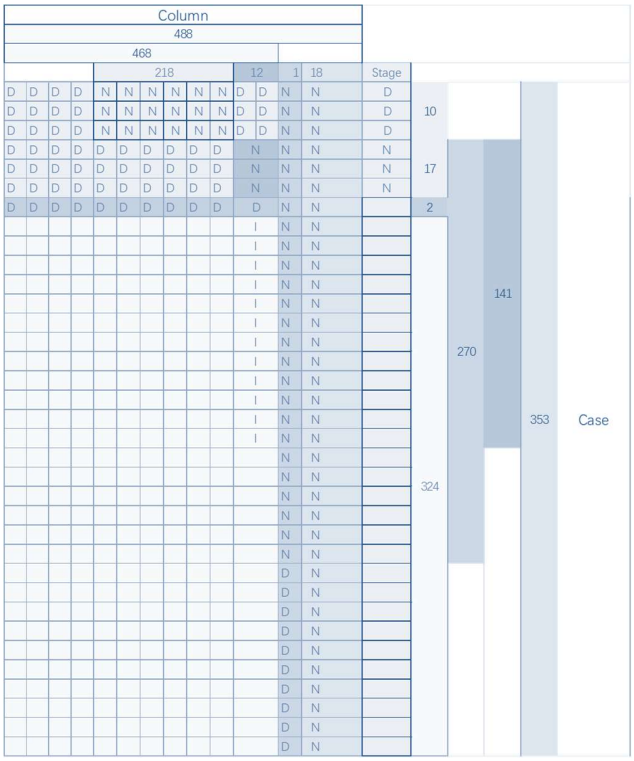

Supplementary Fig. 1. Data Distribution After Processing (D represents drop, N represents NaN value, I represents Imputation)

SUPPLEMENTARY TABLE I
Train and Validation Loss of all AEs

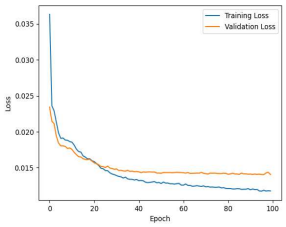

Initial Architecture, 468 Protein Expressions Encode to Dimension of 6

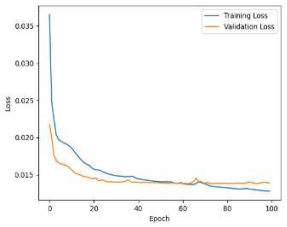

Initial Architecture, 456 Protein Expressions Encode to Dimension of 6

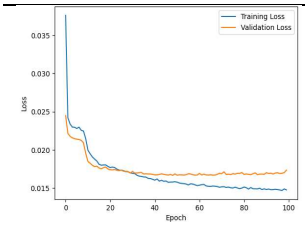

Initial Architecture, 468 Protein Expressions Encode to Dimension of 2

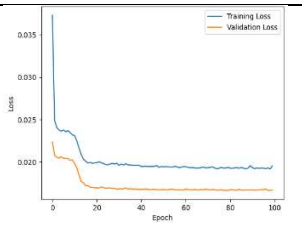

Initial Architecture, 456 Protein Expressions Encode to Dimension of 2

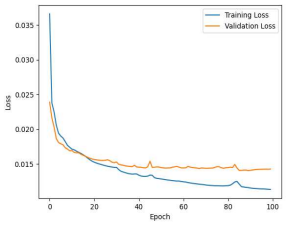

Initial Architecture, 468 Protein Expressions Encode to Dimension of 12

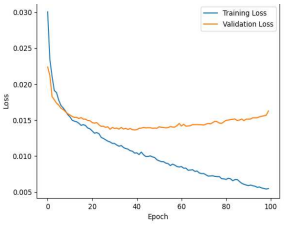

DAE, 468 Protein Expressions Encode to Dimension of 12

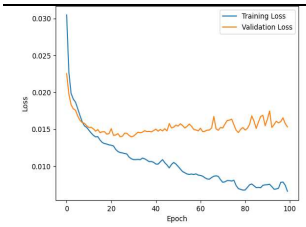

DAE, 468 Protein Expressions Encode to Dimension of 48

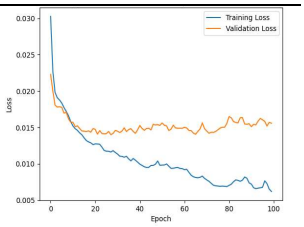

DAE, 468 Protein Expressions Encode to Dimension of 36

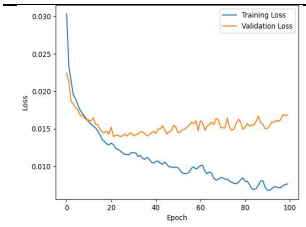

DAE, 468 Protein Expressions Encode to Dimension of 3

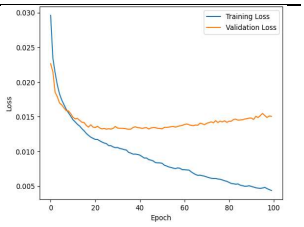

DAE, 468 Protein Expressions Encode to Dimension of 32

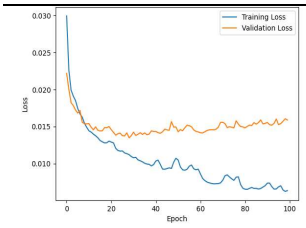

DAE, 468 Protein Expressions Encode to Dimension of 28

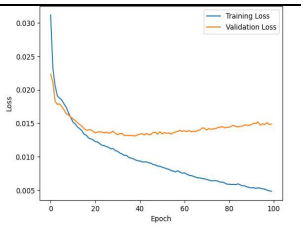

DAE, 468 Protein Expressions Encode to Dimension of 24

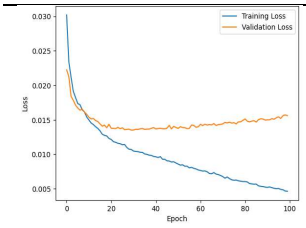

DAE, 468 Protein Expressions Encode to Dimension of 18

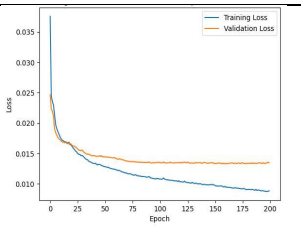

SAE, 468 Protein Expressions Encode to Dimension of 12

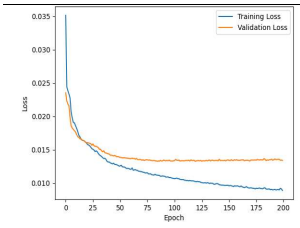

DSAE, 468 Protein Expressions Encode to Dimension of 18

The code of this work is open sourced on GitHub and can be access through https://github.com/smgjch/HSAE.

ACKNOWLEDGMENT

The authors wish to thank Professor D. Fernandez-Reyes for his invaluable support, encouragement, and guidance throughout this research.

REFERENCE

[1] T. Kanazawa, K. Misawa, K. Shinmura, Y. Misawa, G. Kusaka, M. Maruta, T. Sasaki, Y. Watanabe, and T. E. Carey, "Promoter methylation of galanin receptors as epigenetic biomarkers for head and neck squamous cell carcinomas," *Expert Review of Molecular Diagnostics,* vol. 19, no. 2, pp. 137-148, 2019/02/01, 2019.

[2] D. Wu, P. Gong, Q. Zeng, W. Zhang, F. Xie, and X. Zhou, "Prognostic implication of proteomic profiles in head and neck squamous cell carcinoma," *Clinica Chimica Acta,* vol. 509, pp. 304-309, 2020/10/01/, 2020.

[3] R. Abou Khouzam, K. Brodaczewska, A. Filipiak, N. A. Zeinelabdin, S. Buart, C. Szczylik, C. Kieda, and S. Chouaib, "Tumor Hypoxia Regulates Immune Escape/Invasion: Influence on Angiogenesis and Potential Impact of Hypoxic Biomarkers on Cancer Therapies," *Frontiers in Immunology,* vol. 11, 2021-January-20, 2021.

[4] B. Tawk, C. Schwager, O. Deffaa, G. Dyckhoff, R. Warta, A. Linge, M. Krause, W. Weichert, M. Baumann, C. Herold-Mende, J. Debus, and A. Abdollahi, "Comparative analysis of transcriptomics based hypoxia signatures in head- and neck squamous cell carcinoma," *Radiotherapy and Oncology,* vol. 118, no. 2, pp. 350-358, 2016/02/01/, 2016.

[5] A. Košec, R. Novak, P. Konjevoda, V. Trkulja, V. Bedeković, and L. Grgurević, "Tumor tissue hnRNP M and HSP 90α as potential predictors of disease-specific mortality in patients with early-stage cutaneous head and neck melanoma: A proteomics-based study," *Oncotarget; Vol 10, No 62*, 2019.

[6] K. Tan, W. Huang, J. Hu, and S. Dong, "A multi-omics supervised autoencoder for pan-cancer clinical outcome endpoints prediction," *BMC Med Inform Decis Mak,* vol. 20, no. Suppl 3, pp. 129, Jul 9, 2020.

[7] H. Song, C. Ruan, Y. Xu, T. Xu, R. Fan, T. Jiang, M. Cao, and J. Song, "Survival stratification for colorectal cancer via multi-omics integration using an autoencoder-based model," *Exp Biol Med (Maywood),* vol. 247, no. 11, pp. 898-909, Jun, 2022.

[8] R. K. Mondol, N. D. Truong, M. Reza, S. Ippolito, E. Ebrahimie, and O. Kavehei, "AFExNet: An Adversarial Autoencoder for Differentiating Breast Cancer Sub-Types and Extracting Biologically Relevant Genes," *IEEE/ACM Trans Comput Biol Bioinform,* vol. 19, no. 4, pp. 2060-2070, Jul-Aug, 2022.

[9] J. M. Brooks, A. N. Menezes, M. Ibrahim, L. Archer, N. Lal, C. J. Bagnall, S. V. von Zeidler, H. R. Valentine, R. J. Spruce, N. Batis, J. L. Bryant, M. Hartley, B. Kaul, G. B. Ryan, R. Bao, A. Khattri, S. P. Lee, K. U. E. Ogbureke, G. Middleton, D. A. Tennant, A. D. Beggs, J. Deeks, C. M. L. West, J. B. Cazier, B. E. Willcox, T. Y. Seiwert, and H. Mehanna, "Development and Validation of a Combined Hypoxia and Immune Prognostic Classifier for Head and Neck Cancer," *Clin Cancer Res,* vol. 25, no. 17, pp. 5315-5328, Sep 1, 2019.

[10] J. Shao, B. Zhang, L. Kuai, and Q. Li, "Integrated analysis of hypoxia-associated lncRNA signature to predict prognosis and immune microenvironment of lung adenocarcinoma patients," *Bioengineered,* vol. 12, no. 1, pp. 6186-6200, Dec, 2021.

[11] B. Lane, M. T. Khan, A. Choudhury, A. Salem, and C. M. L. West, "Development and validation of a hypoxia-associated signature for lung adenocarcinoma," *Sci Rep,* vol. 12, no. 1, pp. 1290, Jan 25, 2022.

[12] F. Zeng, Y. Zhang, X. Han, M. Zeng, Y. Gao, and J. Weng, "Employing hypoxia characterization to predict tumour immune microenvironment, treatment sensitivity and prognosis in hepatocellular carcinoma," *Computational and Structural Biotechnology Journal,* vol. 19, pp. 2775-2789, 2021/01/01/, 2021.

[13] B. Zhang, B. Tang, J. Gao, J. Li, L. Kong, and L. Qin, "A hypoxia-related signature for clinically predicting diagnosis, prognosis and immune microenvironment of hepatocellular carcinoma patients," *J Transl Med,* vol. 18, no. 1, pp. 342, Sep 4, 2020.

[14] Y. Shou, L. Yang, Y. Yang, X. Zhu, F. Li, and J. Xu, "Determination of hypoxia signature to predict prognosis and the tumor immune microenvironment in melanoma," *Mol Omics,* vol. 17, no. 2, pp. 307-316, Apr 1, 2021.

[15] X. Tian, J. Zheng, W. Mou, G. Lu, S. Chen, J. Du, Y. Zheng, S. Chen, B. Shen, J. Li, and N. Wang, "Development and validation of a hypoxia-stemness-based prognostic signature in pancreatic adenocarcinoma," *Front Pharmacol,* vol. 13, pp. 939542, 2022.

[16] K. Wang, Y. Lu, Z. Liu, M. Diao, and L. Yang, "Establishment and External Validation of a Hypoxia-Derived Gene Signature for Robustly Predicting Prognosis and Therapeutic Responses in Glioblastoma Multiforme," *Biomed Res Int,* vol. 2022, pp. 7858477, 2022.

[17] Z. Liu, Q. Tang, T. Qi, B. Othmane, Z. Yang, J. Chen, J. Hu, and X. Zu, "A Robust Hypoxia Risk Score Predicts the Clinical Outcomes and Tumor Microenvironment Immune Characters in Bladder Cancer," *Frontiers in Immunology,* vol. 12, 2021-August-13, 2021.

[18] C. Nie, H. Qin, and L. Zhang, "Identification and validation of a prognostic signature related to hypoxic

tumor microenvironment in cervical cancer," *PLOS ONE,* vol. 17, no. 6, pp. e0269462, 2022.

[19] J. Zhong, H. Wu, X. Bu, W. Li, S. Cai, M. Du, Y. Gao, and B. Ping, "Establishment of Prognosis Model in Acute Myeloid Leukemia Based on Hypoxia Microenvironment, and Exploration of Hypoxia-Related Mechanisms," *Frontiers in Genetics,* vol. 12, 2021-October-26, 2021.

[20] X. Yang, X. Weng, Y. Yang, M. Zhang, Y. Xiu, W. Peng, X. Liao, M. Xu, Y. Sun, and X. Liu, "A combined hypoxia and immune gene signature for predicting survival and risk stratification in triple-negative breast cancer," *Aging (Albany NY),* vol. 13, no. 15, pp. 19486-19509, Aug 2, 2021.

[21] R. Shi, X. Bao, K. Unger, J. Sun, S. Lu, F. Manapov, X. Wang, C. Belka, and M. Li, "Identification and validation of hypoxia-derived gene signatures to predict clinical outcomes and therapeutic responses in stage I lung adenocarcinoma patients," *Theranostics,* vol. 11, no. 10, pp. 5061-5076, 2021.

[22] Q. Zhang, L. Qiao, J. Liao, Q. Liu, P. Liu, and L. Liu, "A novel hypoxia gene signature indicates prognosis and immune microenvironments characters in patients with hepatocellular carcinoma," *J Cell Mol Med,* vol. 25, no. 8, pp. 3772-3784, Apr, 2021.

[23] D. Chen, H. Huang, L. Zang, W. Gao, H. Zhu, and X. Yu, "Development and Verification of the Hypoxia- and Immune-Associated Prognostic Signature for Pancreatic Ductal Adenocarcinoma," *Front Immunol,* vol. 12, pp. 728062, 2021.

[24] X. Zhang, Y. Li, and Y. Chen, "Development of a Comprehensive Gene Signature Linking Hypoxia, Glycolysis, Lactylation, and Metabolomic Insights in Gastric Cancer through the Integration of Bulk and Single-Cell RNA-Seq Data," *Biomedicines,* vol. 11, no. 11, Nov 1, 2023.

[25] Y. Liu, J. Wu, W. Huang, S. Weng, B. Wang, Y. Chen, and H. Wang, "Development and validation of a hypoxia-immune-based microenvironment gene signature for risk stratification in gastric cancer," *Journal of Translational Medicine,* vol. 18, no. 1, pp. 201, 2020/05/14, 2020.

[26] J. Li, H. Qiao, F. Wu, S. Sun, C. Feng, C. Li, W. Yan, W. Lv, H. Wu, M. Liu, X. Chen, X. Liu, W. Wang, Y. Cai, Y. Zhang, Z. Zhou, Y. Zhang, and S. Zhang, "A novel hypoxia- and lactate metabolism-related signature to predict prognosis and immunotherapy responses for breast cancer by integrating machine learning and bioinformatic analyses," *Frontiers in Immunology,* vol. 13, 2022-October-07, 2022.

[27] Madhumita, and S. Paul, "Capturing the latent space of an Autoencoder for multi-omics integration and cancer subtyping, " *Computers in Biology and Medicine,* vol. 148, pp. 105832, 2022/09/01/, 2022.

[28] J. G. Ellen, E. Jacob, N. Nikolaou, and N. Markuzon, "Autoencoder-based multimodal prediction of non-small cell lung cancer survival," *Scientific Reports,* vol. 13, no. 1, pp. 15761, 2023/09/22, 2023.

[29] A. Arafa, N. El-Fishawy, M. Badawy, and M. Radad, "RN-Autoencoder: Reduced Noise Autoencoder for classifying imbalanced cancer genomic data," *Journal of Biological Engineering,* vol. 17, no. 1, pp. 7, 2023/01/30, 2023.

[30] E. Hoffer, R. Banner, I. Golan, and D. Soudry, "Norm matters: efficient and accurate normalization schemes in deep networks," 03/05, 2018.